Numerical simulations of flow fields through conventionally controlled wind turbines & wind farms

2014 J. Phys.: Conf. Ser. 524 012158

(http://iopscience.iop.org/1742-6596/524/1/012158)

Numerical simulations of flow fields through conventionally controlled wind turbines & wind farms

Ali Emre YILMAZ, Johan MEYERS

Department of Mechanical Engineering, KU Leuven, Celestijnenlaan 300A – bus 2421, B3001 Leuven, Belgium.

E-mail: aliemre.yilmaz@kuleuven.be, johan.meyers@kuleuven.be

Abstract. In the current study, an Actuator-Line Model (ALM) is implemented in our in-house pseudo-spectral LES solver SP-WIND, including a turbine controller. Below rated wind speed, turbines are controlled by a standard-torque-controller aiming at maximum power extraction from the wind. Above rated wind speed, the extracted power is limited by a blade pitch controller which is based on a proportional-integral type control algorithm. This model is used to perform a series of single turbine and wind farm simulations using the NREL 5MW turbine. First of all, we focus on below-rated wind speed, and investigate the effect of the farm layout on the controller calibration curves. These calibration curves are expressed in terms of non-dimensional torque and rotational speed, using the mean turbine-disk velocity as reference. We show that this normalization leads to calibration curves that are independent of wind speed, but the calibration curves do depend on the farm layout, in particular for tightly spaced farms. Compared to turbines in a lone-standing set-up, turbines in a farm experience a different wind distribution over the rotor due to the farm boundary-layer interaction. We demonstrate this for fully developed wind-farm boundary layers with aligned turbine arrangements at different spacings (5D, 7D, 9D). Further we also compare calibration curves obtained from full farm simulations with calibration curves that can be obtained at a much lower cost using a minimal flow unit.

1. Introduction

Modeling approaches such as the Actuator Disc Model (ADM) and the Actuator Line Model (ALM) [1] are quite common for the representation of wind turbines in wind farm simulations. With these models, boundary layer over the turbine geometries is not required to be resolved since the turbine induced forces are calculated as integral quantities. Thus, the grid density required by these models is not much larger than the ones required for the Large Eddy Simulation (LES) of atmospheric boundary layers and even large wind farm simulations can be performed with an acceptable computational time and cost. In addition to their computational efficiencies, these models also provide reliable results [2]. When studying overall wind-farm boundary layer interaction, ADMs are often sufficient. However, to study the near wake effects, tip vortices, and in particular to study effects of turbine control, an actuator line model is necessary [3].

An ALM distributes turbine induced forces along lines that are representing the turbine blades. This representation gives the advantage of controlling rotational speed and blade pitch angles of the

turbines in the simulations as it is in the real cases, hence, making the model a seamless choice for the controller studies.

Except for startup and emergency shutdown cases, the goal of the controller systems essentially consists of extracting more power in moderate wind speeds and limiting rotational speed at high wind speeds preventing damage to components. The former is generally achieved by changing the generator resisting torque in order to adapt the rotational speed of the rotor proportional to the wind speed. The latter is achieved by pitching the blades towards off-design positions, in turn decreasing the aerodynamical torque acting on the rotor.

For the control of wind turbines in moderate wind speeds, the optimal operating point is an input to the generator torque controller and required to be known before the operation. Hence, the turbine can trace this point maximizing its power production. However, it is not so easy to estimate the optimal operating point accurately from tests and simulations. Therefore, on site turbines can easily be driven towards non-optimal operating conditions [4]. In addition to erroneous estimates, the optimal operating point might also be dependent on the farm layout. In such a case, an optimal point defined for a single turbine in clean free stream conditions could cause the same wind turbine to operate under non-optimal conditions in the farm layout. In a field like wind energy, where even 1% of power production has significant importance, this issue should be investigated.

In this study, an ALM model is implemented to an in-house pseudo-spectral LES solver. For the operation in moderate wind speeds, a standard torque controller is employed to regulate the rotational speed of the rotor for maximum power extraction. In high wind speeds, the rotational speed of the rotor is controlled by a blade pitch controller based on a proportional-integral (PI) type controller algorithm. Within this framework, first, a set of simulations are performed so as to examine the operation of the controllers in response to the changing wind speeds. Later, the effect of the wind farm layout on optimal operating point is investigated. For that purpose, a minimal flow unit approach to be used in infinite wind farm simulations is introduced.

The paper is further organized as follows. First in Section 2, theory of ALM and the controllers are explained. Subsequently, in Section 3, results are presented and discussed. Finally, conclusions are presented in Section 4.

2. Theory

2.1. Simulation Suite

The framework that is used in this study is an in-house LES solver, SP-WIND. It solves the filtered Navier-Stokes equations. In horizontal directions spatial discretization is based on pseudospectral methods while for the vertical direction finite differences are used. In the horizontal directions the boundary conditions are periodic. At the bottom face of the domain, a wall stress boundary condition is applied [5]. At the top surface, a symmetry boundary condition is used. The flow field is driven in the axial direction by a constant pressure gradient, and updated in time with a four-stage Runge-Kutta scheme. Details of the framework can be found in references [5], [6]. Also a very similar code is used in reference [2]. In the simulations of wind farms, turbines are modeled by an Actuator Line Model (ALM), and turbine-induced forces are added to the momentum equations as body forces.

2.2. Actuator Line Model

In an ALM, each turbine blade is represented as a line, and forces are calculated at a number of discrete points along this line. To that end, the blade cross sections at each discrete point are considered. These cross sections consist of airfoils on which forces are calculated from tabulated lift and drag coefficients. Since the effect of the boundary layer is already included implicitly in the aerodynamic force coefficients, the model does not require fine meshes around the blades to resolve the boundary layer.

The angle of attack that each section along the blade sees is calculated from the local velocity components, rotational speed of the rotor and the local pitch angle of the section. We assume two

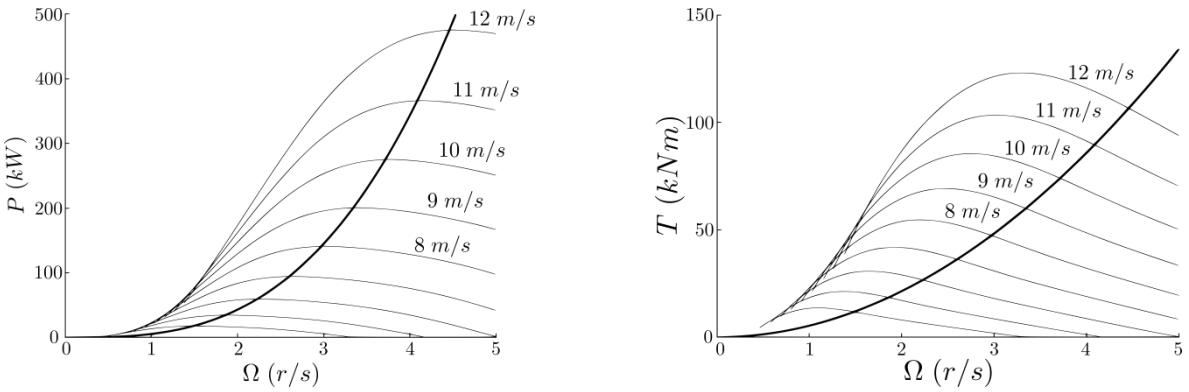

Figure 1 Typical power, torque vs. rotational speed curves for HAWTs [7].

dimensional flow, and neglect the radial component of the local velocity vector. Once the angle of attack of the blade section is obtained, turbine induced forces are calculated from the airfoil aerodynamical data and added to the flow field.

Although it is not necessary to resolve the boundary layer, the model still requires a finer grid than the LES grid in order to resolve the turbine geometry properly. In this direction, each blade is discretized by 50 points. Subsequently, turbine induced forces are calculated on this finer grid using a velocity field that is linearly interpolated from the LES grid. Finally, calculated forces are distributed back to the LES grid by a Gaussian filter [6]. In addition to the blades, the nacelle is also discretized (using 30 points) and represented as a drag disc with a drag coefficient of 1.0.

At the tip of the blades, flow leaks from the high-pressure lower surface to the low-pressure upper surface. This creates a three dimensional flow near the tip, that is not well modelled by the two-dimensional flow approach explained above. In order to correct the forces in the near-tip region a tip correction [8] is applied directly to the airfoil data.

2.3. Controller

Modern large wind turbines adapt themselves to the changing wind speeds by means of controllers. In the operating range of turbines, there are three regions based on the strength of the wind speed. Region I is the startup phase. Wind speed in this region is not high enough for maintaining the power extraction and continuous rotation of the rotor at the same time. The most common control approach in this region is setting the blades to maximum torque positions without applying any resisting torque from the generator, resulting in free rotation without power production. Here, the aim of the controller is just accelerating the rotor to a minimum rotational speed after which generator torque controller intervenes.

2.3.1. Region II Controller (Generator Torque Controller)

After its rotor exceeds the minimum rotational speed threshold, the turbine starts extracting power. In this region, the aim of the controller is to extract as much power as possible from the wind by changing the rotational speed of the rotor in response to changes in the wind speed. This is generally achieved by controlling the generator resisting torque.

Figure 1 shows a typical change of power and rotor aerodynamical torque of a horizontal axis wind turbine (HAWT) as function of rotational speed and for different wind speeds. The solid curve represents the loci of maximum power. These curves are the characteristics of the turbine and known from field tests, wind tunnel studies, numerical simulations etc. Once these characteristics are known, the turbine torque is controlled such that it follows the locus of maximum power curve on torque vs. rotational speed plot. This is explained in the following paragraphs.

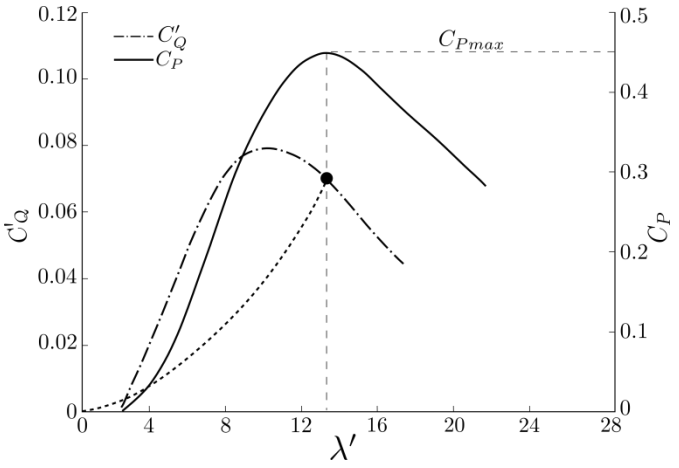

Figure 2 Typical non-dimensional power and torque vs. rotational speed curves for HAWTs.

As long as the tip speed ratios of two geometrically similar turbines are the same, and the upstream wind field is the same, the local flow field around those wind turbines must also be similar [9]. As a result, with the proper nondimensionalization of torque and rotational speed, curves corresponding to different wind speeds in figure 1 can be collapsed onto a single curve, reducing the curve with the loci of maximum power to an optimal operating point. This is usually achieved by using the free stream velocity as the reference. However, the definition of the free stream velocity in a wind farm is ambiguous. Therefore, we will nondimensionalize torque and rotational speed with the disk-based velocity instead, leading to

$$C'_Q = \frac{T}{{}^1\!/_2 \rho U_d^2 A_d d} \quad , \quad \lambda' = \frac{\omega R}{U_d} \tag{1}$$

Where, T is the torque, ρ the density, U_d the disc averaged velocity, d the rotor diameter, ω the rotational speed and A_d the disc area. Note that for further discussion, the power is nondimensionalized by the free stream velocity, and not the disc velocity. In fact, normalization of a power coefficient with disk velocity shifts the maximum of the curve away from the true optimal operating point. Typical non-dimensional power (C_p), torque (C'_Q) and rotational speed (λ') curves of a HAWT are shown in figure 2. Here, the optimal operating point is denoted by a dot on the C'_Q-λ' curve.

Below rated wind speed (region II), C'_Q-λ' curves can be used for generator-torque control. The duty of the generator torque controller is to maintain optimal operation conditions. This can be achieved by simply employing Newton's 2nd law, with some manipulations. This is explained in the following.

There are mainly two torque components acting on the rotor; one of them is the aerodynamical torque that is coming from the wind while the other one is the resisting torque coming from the generator. From Newton's second law, the net torque acting on the rotor equals the rotational inertia (J) times the angular acceleration ($\dot{\omega}$), i.e. $T = J\dot{\omega}$. Combining this with (1) and rearranging leads to

$$T = \rho \omega^2 R^5 \pi \frac{C'_Q}{\lambda'^2} \tag{2}$$

Both the aerodynamical and generator torques can be defined in terms of this expression.

In figure 2, the dash-dotted curve (C'_Q) represents all possible operating points of the turbine. The aerodynamical torque acting on the turbine rotor can be calculated from (2) for all those operating points. Moreover, we assume that generator is applying a resisting torque (T_{gen}) that corresponds to the optimal operating point (C'^*_Q) on the turbine's C'_Q-λ' curve, then from (2),

$$T_{gen}(\omega) = \rho\omega^2 R^5 \pi \frac{C_Q'^*}{\lambda_*'^2} \tag{3}$$

In (3), the only variable required for the control is the rotational speed which can easily be measured during the operation. It is straightforward to show that the generator torque using (3) pushes the turbine to its optimal operating point in response to varying wind speeds. This is explained in the following paragraphs.

Substituting (2) and (3) into Newton's 2nd law and manipulating, one can express the rotational acceleration as follows

$$\dot{\omega} = \frac{\rho\omega^2 R^5 \pi}{J\lambda'^2}\left(C_Q' - \frac{C_Q'^*}{\lambda_*'^2}\lambda'^2\right) \tag{4}$$

In this expression, the factor in front of the parenthesis is always positive. Therefore, the sign of the angular acceleration of the rotor equals the sign of the term in parenthesis. In figure 2, the second (quadratic) term inside the parenthesis in (4) is plotted as the dotted curve. We now observe that to the left of the optimal operating point, C_Q' is always larger than this quadratic term (except at very low speeds, i.e. region I). As a consequence, the rotor will accelerate in this region up to the optimal operating point. Once the turbine reaches the optimal operating point, the angular acceleration becomes zero and turbine remains in this point. For the operating points that fall to the right hand side of the optimal point, a similar analysis holds, i.e. the turbine will decelerate back to the optimal operating point. This type of control is known as *standard-torque-control* [10] and used in the scope of this study.

2.3.2. Region III Controller (Blade Pitch Controller)

In region III where the wind speed is above the rated value, the aim of the controller is to prevent the rotational speed of the rotor going beyond the electro-mechanical limits. Since the generator resisting torque is already at its rated value and has no excess torque in this region, it is not possible to regulate the rotational speed with the same methodology as used for region II in 2.3.1.

For maximum power extraction purposes the optimal blade pitch setting in region II is around zero degrees. Control in region III is basically achieved by pitching the blades either towards feather or stall, reducing the aerodynamic torque acting on the rotor [11]. In the current study, a collective pitch-to-feather approach is employed. For this purpose, a PI type control algorithm [12] is used with an infinite pitch rate.

$$\beta(t) = K_c\left[\omega_e(t) + \frac{1}{T_i}\int_0^t \omega_e(t)dt\right], \tag{5}$$

where β is the blade pitch angle, ω_e the rotational speed error, t the time, and K_c and T_i are two case specific parameters that need to be tuned.

In tuning the controller parameters, one must know the process characteristic in advance. This can be achieved by simply bumping the pitch angle first and then analyzing the response of the rotational speed. Once the process characteristics are explored, and depending on these characteristics, one of the suitable tuning rules such as Cohen-Coon, Lambda, Ziegler-Nicholas etc. can be used for tuning the controller parameters. An extensive explanation of PI controllers and tuning of the controller parameters can be found in references [12], [13].We note that, the tuning parameters are dependent on the free stream velocity. For the wind turbines operating in a wide range of wind speeds in region III, controller tuning has to be done separately for a number of reasonably different wind speeds. Hence,

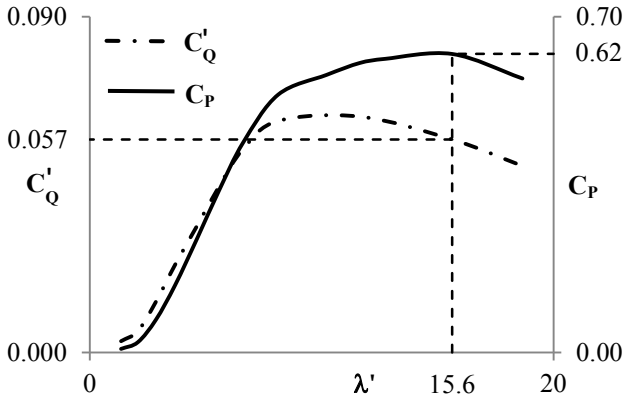

Figure 3 NREL-5MW turbine characteristics.

the controller can adapt itself to a variety of different wind speeds by dynamically changing its parameters. This type of adaptation known as *gain scheduling* is not applied in this study.

3. Results

In the current study, we have three main objectives. First of all, we verify the implemented turbine model (ALM) and the controllers for different wind speeds (cf. §3.1). Secondly, we identify minimal flow units, that can be used to calibrate C_Q'-λ' curves (cf. §3.2). Lastly, we investigate wind-farm layout effects on the C_Q'-λ' curves (cf. §3.3).

In all simulations, the NREL-5MW turbine [14] is modeled and used. In stand-alone wind turbine simulations, the domain length is kept reasonably long (60d in x and 10d in y direction) in the horizontal plane to minimize the effect of periodicity of our spectral method. In the vertical direction, the domain height is one kilometer. The turbine rotor area is resolved approximately by 100 (10×10) grid points. In the axial direction, the grid spacing is set approximately to 1/6 of the rotor diameter in order to capture the dominant turbulent structures adequately. In the wind farm simulations, the grid density is kept almost the same. However, except for the z-direction, dimensions of the domain are decided by the turbine spacing and the size of the farm.

3.1. Verification of the controllers

Operation of the region II controller requires the knowledge of turbine specific optimal operating conditions in advance. For this purpose, several cases with different tip speed ratios are simulated without activating the controller. Results are given in figure 3. It is observed that the optimal operating point of the NREL-5MW turbine is given by a torque coefficient of 0.057 and a corresponding optimal tip speed ratio of 15.6. We remark that there is an issue with the power coefficient, which attains a value that is too high compared to the Betz limit (cf. the maximum value of 0.62 in the figure). We expect that this is a matter of calibration of the wind turbine model, and currently, we are trying to improve the results. For now, the optimal C_Q'-λ'operating point is used as an input to the region II controller in the subsequent simulations. In addition, the region III controller gain and integral time are also tuned, yielding 1.07 and 0.056s respectively.

With these settings, another set of simulations is performed with a controlled stand-alone wind turbine. Results are shown in figure 4. In the first ninety computational time units, the free stream velocity is kept below rated. During this period, the generator torque controller regulates the rotational speed on its own in a turbulent fluctuating field, keeping the power coefficient maximum. Starting from t=90 the wind speed is gradually increased, and the blade pitch controller starts to intervene, preventing the rotor to accelerate over the rated rotational speed.

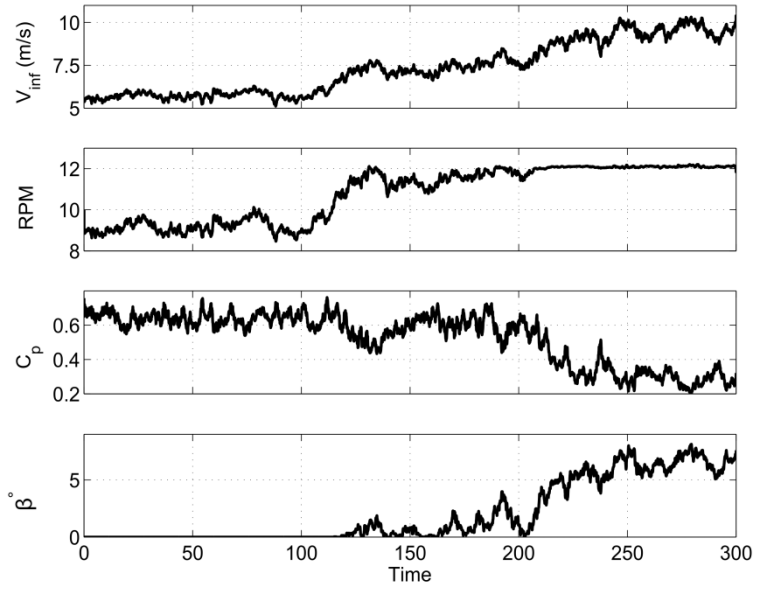

Figure 4 Controlled operation of NREL-5MW turbine below and above rated conditions.

From t=180 onwards, the free stream velocity is above rated. At this point, the blade-pitch-controller pitches the blades to keep rotational speed at its rated value, while at the same time, causing a significant drop in the power coefficient. It should be noted here that in figure 4 the rated rotational speed is reached at a lower free stream velocity than it is reported in [14]. Also the rated power is different from the 5MW that is expected for the NREL turbine. This is directly linked with the problems discussed in figure 3, i.e. a power coefficient that is too high.

So far we have studied the stand-alone wind turbine cases. Optimal operation setting of a stand-alone wind turbine could also be used for the control of the same turbine in the wind farm case requiring that it is not sensitive to the farm layout. The following sections look for an answer to this question.

3.2. Minimal flow unit approach for the control studies of wind farms

In order to sustain the turbulence in a simulation with periodic boundary conditions, there is a lower limit on the size of the computational domain [15]. Using 'infinite' wind farms (with periodic boundary conditions), and turbine spacing of 7D by 5D, it necessary to work with at least 10×6 turbines in the simulations, when exploring the effect of wind farm layouts on C_Q'-λ' curves. However, the simulation of such large wind farms is computationally expensive. Therefore, here we are looking for the smallest domain for which C_Q'-λ' curves can be reproduced without losing too much accuracy.

C_Q' and λ' are two integral quantities that are averaged in time. For that reason, sustainability of detailed large-scale turbulent structures in the simulation domain may not be of dominant importance for the determination of C_Q'-λ' curves. To verify this, several simulations are performed with a 10×6 wind farm and with its 1×1 minimal flow unit separately. This is demonstrated in figure 5 (left). In the minimal flow unit case, C_Q'-λ' curves are obtained by averaging the values over time after reaching the statistically stationary state. In the wind farm cases, in addition to the former, the values are also averaged over the turbines. Minimal flow unit simulations are conducted on 8 processors, while 32 processors are used for the full wind farm simulations. A comparison of the results is presented in figure 5 (right). It shows that, C_Q'-λ' curves obtained by the minimal flow unit simulation are in good agreement with the wind farm simulations. As a result, minimal flow unit simulations can be used as a replacement for the wind farm simulations in producing such data. Hence, in the study of the layout effect on the turbine C_Q'-λ' curves we continue with the minimal flow unit simulations.

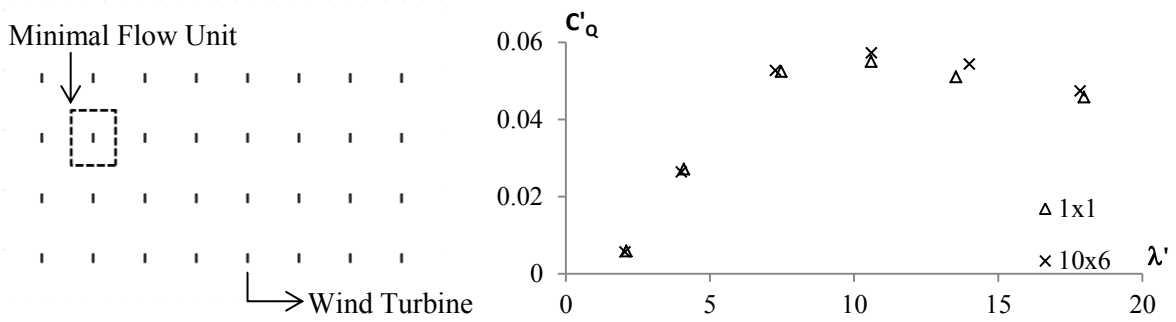

Figure 5 Wind farm and its minimal flow unit (left), and comparison of minimal flow unit and wind farm simulation results (right).

3.3. Effect of wind farm layout on turbine C_Q'-λ' curves

We start this subsection first by investigating the effect of the free stream velocity on the C_Q'-λ' curves of a wind turbine in a wind farm. For this purpose, three sets of simulations, each at different wind speeds, are performed with a 1×1 infinite wind farm. In the simulations, the free stream velocity experienced by the wind turbines is changed by manipulating the pressure gradient in the axial direction (dpdx). Results of the simulations are presented in figure 6. It is shown that C_Q'-λ' curves of a wind turbine in a wind farm perfectly match for different wind speeds.

Next, the influence of the wind farm layout is investigated by performing a series of simulations with aligned wind farms. In this direction, several wind farm cases with different axial and span-wise distances between the wind turbines are simulated. Results are presented in figure 7. Different span-wise distances between the wind turbines in a wind farm are shown to have no significant effect on the turbines' C_Q'-λ' curves. On the other hand, the axial distance between the wind turbines has an influence that cannot be ignored. Moreover, this influence becomes more remarkable as the turbine spacing is decreased. This proves that, geometric similarity of the individual wind turbines, together with the equality of the tip speed ratios, are not sufficient to sustain similar flows through the wind farms. Instead, individual turbine geometry and the farm layout -at least in the main flow direction- must be considered as a whole with regard to the geometric similarity when dealing with the wind farm flows.

4. Conclusions

In the scope of this study an Actuator Line Model and region II&III controllers are implemented to an in-house LES solver. Within this framework several stand-alone wind-turbine and wind-farm simulations are performed with the NREL-5MW turbine. We find that ALM works seamlessly but has some accuracy issues that require calibration.

We further showed that wind farm layout has an influence on the C_Q'-λ' calibration curve that are typically used for control. In particular the spacing in the axial direction is of importance.

We also investigated the use of a minimal flow unit approach to calibrate C_Q'-λ' curves. We found that C_Q'-λ' curves can be produced reasonably accurate by using a minimal flow unit.

Acknowledgements

The authors acknowledge support from the European Research Council (FP7-Ideas, grant no.306471) the Research Foundation - Flanders (FWO, grant no. G.0376.12). Simulations were performed on the computing infrastructure of the VSC (Flemish Supercomputer Center), funded by the Hercules foundation.

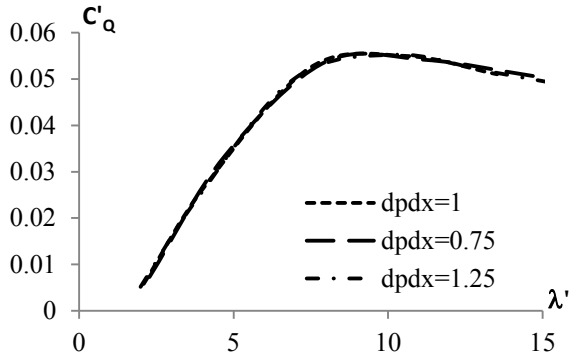

Figure 6 Effect of free stream velocity on dimensionless torque-rotational speed curves of wind turbines in aligned wind farm layout.

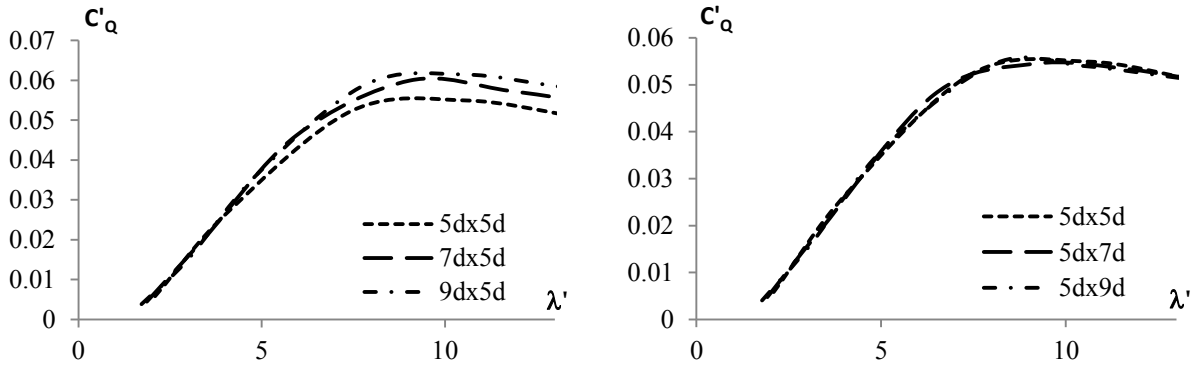

Figure 7 Effect of axial (left) and span-wise (right) turbine spacing on dimensionless torque-rotational speed curves of wind turbines in aligned wind farm layout.

References

[1] J. N. Sørensen and W. Z. Shen, "Numerical Modeling of Wind Turbine Wakes," *J. Fluids Eng.*, vol. 124, no. 2, p. 393, 2002.

[2] F. Porté-Agel, Y.-T. Wu, H. Lu, and R. J. Conzemius, "Large-eddy simulation of atmospheric boundary layer flow through wind turbines and wind farms," *J. Wind Eng. Ind. Aerodyn.*, vol. 99, no. 4, pp. 154–168, Apr. 2011.

[3] B. Sanderse, "Review of computational fluid dynamics for wind turbine wake aerodynamics," no. February, pp. 799–819, 2011.

[4] K. E. Johnson, "Adaptive Torque Control of Variable Speed Wind Turbines," 2004.

[5] J. Meyers and C. Meneveau, "Large eddy simulations of large wind-turbine arrays in the atmospheric boundary layer," in *AIAA Paper*, 2010, no. January.

[6] M. Calaf, C. Meneveau, and J. Meyers, "Large eddy simulation study of fully developed wind-turbine array boundary layers," *Phys. Fluids*, vol. 22, no. 1, p. 015110, 2010.

[7] F. D. Bianchi, H. De Battista, and R. J. Mantz, *Wind Turbine Control Systems*. Springer, 2007.

[8] W. Z. Shen, R. Mikkelsen, J. N. Sørensen, and C. Bak, "Tip loss corrections for wind turbine computations," *Wind Energy*, vol. 8, no. 4, pp. 457–475, Oct. 2005.

[9] J. Manwel, J. McGowan, and A. Rogers, *Wind Energy Explained*, 2nd ed. John Wiley&Sons Ltd, 2009.

[10] L. Y. Pao and K. E. Johnson, "A tutorial on the dynamics and control of wind turbines and wind farms," *2009 American Control Conference*, 2009. [Online]. Available: http://ieeexplore.ieee.org/lpdocs/epic03/wrapper.htm?arnumber=5160195.

[11] T. Burton, N. Jenkins, D. Sharpe, and E. Bossanyi, *Wind Energy Handbook*, 2nd ed. UK: John Wiley & Sons, Ltd, 2011.

[12] Jacques F. Smuts, *Process Control for Practitioners*. OptiControls Inc., 2011.

[13] W. Altmann, *Practical Process Control for Engineers and Technicians*. Elsevier Science, 2005.

[14] J. Jonkman, S. Butterfield, W. Musial, and G. Scott, "Definition of a 5-MW Reference Wind Turbine for Offshore System Development," 2009.

[15] J. Jiménez and P. Moin, "The minimal flow unit in near-wall turbulence," *J. Fluid Mech.*, vol. 225, pp. 213–240, 1991.